encit 2020

ABCM Associação Brasileira de Engenharia e Ciências Mecânicas

18th Brazilian Congress of Thermal Sciences and Engineering
November 16-20, 2020 (Online)

ENC-2020-0062
INFLUENCE OF THE FIRE SOURCE POSITION ON THE HOT GAS LAYER TEMPERATURE IN A MULTI-COMPARTMENT SCENARIO

Rodolfo Prediger Helfenstein
Programa de Pós-Graduação em Engenharia Mecânica (PROMEC), Universidade Federal do Rio Grande do Sul - (UFRGS) – Rua Sarmento Leite, n. 425, CEP 90050-170, Porto Alegre, RS, Brasil
rodolfo.helfenstein@ufrgs.br

Calisa Katiuscia Lemmertz
Programa de Pós-Graduação em Engenharia Mecânica (PROMEC), Universidade Federal do Rio Grande do Sul - (UFRGS) – Rua Sarmento Leite, n. 425, CEP 90050-170, Porto Alegre, RS, Brasil
calisa.lemmertz@ufrgs.br

Felipe Roman Centeno
Programa de Pós-Graduação em Engenharia Mecânica (PROMEC), Universidade Federal do Rio Grande do Sul - (UFRGS) – Rua Sarmento Leite, n. 425, CEP 90050-170, Porto Alegre, RS, Brasil
frcenteno@mecanica.ufrgs.br

Abstract. *The use of computational fluid dynamics (CFD) models is becoming the main method to predict and reconstruct fire behavior. The Hot Gas Layer Temperature (HGLT) is one of the most important parameters in compartment fires, once it is the temperature of the room that determines the impact and development of the fire. Thus, the present work aims to analyze numerically, using the software Fire Dynamics Simulator (FDS), the influence of the fire source location on the Hot Gas Layer Temperature in a multi-compartment fire. The numerical model was validated by comparing the results obtained through FDS with the experimental data described by Johansson et al. (2015), showing a good agreement. The results showed that when placing the fire source next to a wall or a corner, the HGLT in the fire room increases while in the adjacent room it decreases, due to the reduction of the air entrainment and the thickness of the smoke layer. The highest HGLT in the fire room occurred when the pool fire was positioned in a corner (P.3), while in the adjacent room the highest HGLT was found when the pool fire was positioned in the center of the scenario 1 room.*

Keywords: *Multi-compartment fires, FDS, Hot Gas Layer Temperature, fire source position*

1. INTRODUCTION

The use of computational fluid dynamics (CFD) models is becoming the main method to predict and reconstruct fire scenarios. These CFD models solve simultaneously the equations that mathematically model the conservation principles involved in the problem. There is a wide range of engineering processes where CFD models can be employed, including heat transfer, fluid flow, combustion and chemical reactions.

A fire in one or more compartments can develop in different ways, depending on the characteristics of the environment, due to the fire being a highly interactive phenomenon. According to Karlsson and Quintiere (2000), the factors that influence the fire development in compartments are the geometry of the compartment and openings, the properties of the walls and ceiling materials, the size and location of the ignition source.

During a pre-flashover fire, the combustion process releases energy in the form of heat, in addition to a variety of chemical products, including toxic and non-toxic gases and particles. This causes an increase in the temperature of the combustion products, decreasing their density, and causing the hot gases to rise towards the ceiling, forming a plume that entrains cold air that surrounds it. Cold air is carried by the plume, decreasing its temperature and increasing its volume.

The plume rises until it impinges on the ceiling, spreading along it until it reaches the compartment walls, being forced to move downwards, forming two distinct layers: one located at the lower of the compartment (cold layer), which is rich in fresh air and has a lower temperature, and another, at the upper part of the compartment (hot layer), which is rich in combustion products and has a higher temperature. This stratification of the room gases in two distinct layers is widely known as The Two-Zone Model.

Due to the mass flow provided by the fire plume, its thickness will continue to increase until it finds an opening that connects it to an adjacent room. The hot gases will flow through this opening, moving towards the ceiling of the adjacent room and spreading through it until they reach the walls, forming two distinct layers in the adjacent room. As the hot gas layer thickness increases, it will find an opening that connects it to the external environment, leaving the compartment. According to Marchetti (2012), the HGLT is one of the most important parameters that a fire model can predict, because it is the room temperature that will determine the impact of a fire and its influence on the Heat Release Rate (HRR) and fire spread in the room.

Due to the large number of variables and the complexity of the phenomenon, several authors have studied experimentally and numerically fire dynamics in compartments. These studies seek to understand and quantify the influence of certain parameters on the development and behavior of the fire. As an example of these parameters, the position of the heat source, the size of the compartment and the ventilation factor can be mentioned.

Tlili *et al.* (2016) conducted a numerical investigation of fire induced airflow in a compartment to verify the influence of the source location on the mass flow rate at the exit doorway and on the thermal flow field. The results showed that the height of the heat source has a significant impact on the temperature field and the layer interface. Based on these results, they established a mathematical correlation to calculate the mass flow rate at the doorway according to the three-dimensional coordinates of the heat source within the fire room.

Sahu *et al.* (2017) investigated, numerically and experimentally, the behavior of diesel pool fires in a large-scale compartment under different door open conditions. The experimental results showed that the burning behavior changes significantly as oxygen availability gets limited. Also, the heat release rate was found to be higher in half door open condition, in which the thermal feedback dominates the fuel burning rather than the oxygen availability reduction. The numerical results showed a good agreement with experimental data.

Węgrzyński and Konecki (2018) analyzed the mass and temperature of smoke inside and outside a compartment, considering as variables the locations of the fire and the size of the compartment. A numerical model was applied to estimate the mass flow (in and out) in different compartment configurations, using a scale model to validate the numerical simulations. They concluded that the size of the compartment and the fire location within the room do not influence the mass flow of the smoke in a considerable way. However, the smoke temperature changes considerably with the variation of both parameters. The highest temperature was measured at the smallest compartments and for the fires furthest away from the opening. In very large compartments a lower average temperature of the smoke layer was observed, however, higher peaks of local temperature were measured. It was observed that, in these large compartments, as long as the plume was not disturbed by incoming air, the position of the fire did not influence the smoke average temperature temperatures.

Lemmertz *et al*. (2018) analyzed the influence of the fire source location (longitudinal, transversal and elevation) on the HGLT in pre-flashover compartment fires, in order to determine the most dangerous fire scenario based on the fire source location. The results showed that the transversal and longitudinal fire position does not affect considerably the temperature, except when the fire was placed near a wall or a corner. The elevation of the fire source showed an important influence on the results, a significant increase on the hot gas layer and the maximum temperatures, as well as in the interface layer height was observed.

Betting *et al.* (2019) investigated the dynamics of smoke in a confined environment through a double approach, where the experimental data of the temperature and speed fields were recorded and analyzed, being compared with the numerical results obtained through simulations carried out in FDS. The results showed that FDS is able to reproduce both temperature and velocity data with precision depending on the heat release rate and the room volume.

Haouari-Harrak *et al.* (2020) investigated the impact of the room aspect ratio on the smoke filling time in the case of fire plume by means of full scale simulations in order to evaluate the two-zone models. The results showed that the two-zone model overestimates the smoke filling time in the case of a compartment with a large surface area. The zone model results were improved by establishing correlations for the duration of each phenomena occurring before the formation of two-layer stratification in a fire compartment.

Thus, the present work aims to evaluate the ability of the Fire Dynamics Simulator (FDS) software to numerically reproduce fires in multi-compartments, and after that, this work analyses the influence of the fire source location (at the floor level) on the Hot Gas Layer Temperature (T_U) in pre-flashover multi-compartment fires, in order to determine the worst scenario possible, so that it can be taken into account by fire safety engineers during the analysis of a case or in the design of fire safety projects.

2. NUMERICAL METHOD

2.1 Governing equations

FDS is a computational fluid dynamics (CFD) software that is described as a "fire model". It solves numerically a form of the Navier-Stokes equations for low Mach numbers, with an emphasis on transporting smoke and heat from fires. The set of equations that mathematically describe the fire phenomenon in a compartment are the mass

conservation equation, transport equation for each lumped species, momentum conservation equation, energy conservation equation and the equation of state.

Mass conservation equation

$$\frac{\partial \rho}{\partial t} + \nabla.(\rho \boldsymbol{u}) = \dot{m}_b{}''' \tag{1}$$

Transport equation for each lumped species

$$\frac{\partial}{\partial t}(\rho Z_\alpha) + \nabla.(\rho Z_\alpha \boldsymbol{u}) = \nabla(\rho D_\alpha \nabla Z_\alpha) + \dot{m}_\alpha{}''' + \dot{m}_{b,\alpha}{}''' \tag{2}$$

Momentum conservation equation

$$\frac{\partial}{\partial t}(\rho \boldsymbol{u}) + \nabla.\rho \boldsymbol{u}\boldsymbol{u} + \nabla p = \rho \boldsymbol{g} + \mathbf{f}_b + \nabla.\tau_{ij} \tag{3}$$

Energy conservation equation

$$\frac{\partial}{\partial t}(\rho h_s) + \nabla.(\rho h_s \boldsymbol{u}) = \frac{D\overline{p}}{Dt} + \dot{q}''' + \dot{q}_b{}''' - \nabla.\left(-k\nabla T - \sum_\alpha h_{s,\alpha}\rho D_\alpha \nabla Z_\alpha + \boldsymbol{q}_r{}''\right) \tag{4}$$

Equation of state

$$\bar{p} = \frac{\rho T R}{\bar{W}} \tag{5}$$

where ρ is the specific mass, t is the time, $\boldsymbol{u}$ is the velocity vector, $\dot{m}_b'''$ is the source term of mass, Z_α is the species mixture fraction, D_α is the diffusion coefficient, $\dot{m}_\alpha{}'''$ is the mass production rate per unit volume of species α by chemical reactions, p is the pressure, $\boldsymbol{g}$ is the gravity vector, $\mathbf{f}_b$ represents the drag force exerted by the subgrid-scale particles and droplets, τ_{ij} is the viscous stress tensor, h_s is the sensible enthalpy, $\bar{p}$ the background pressure, $\dot{q}_b'''$ is the energy transferred for particles and droplets of sub-mesh scale, k is the thermal conductivity, T is the temperature, R is the universal gas constant and $\bar{W}$ the molecular weight of the gas mixture.

2.2 Combustion and radiation models

Combustion is simulated based on the mixing-limited, infinitely fast reaction of lumped species, being the heat release rate per unit area defined as the product of the sum of the lumped species mass products rates and their respective heat of formation. Combustion is introduced into the energy conservation equation via the source term $\dot{q}'''$.

$$\dot{q}''' = -\sum_\alpha \dot{m}_\alpha{}''' \Delta h_{f,\alpha} \tag{6}$$

Thermal radiation is calculated using the radiative transfer equation (RTE) for a non-scattering gray gas, being solved by a technique that is similar to the finite volume method. This term is introduced into the energy equation via the source term $\dot{q}_r{}'''$.

$$\dot{q}_r{}''' \equiv -\nabla.\dot{\boldsymbol{q}}_{\boldsymbol{r}}{}''(\boldsymbol{x}) = \kappa(\boldsymbol{x})[U(\boldsymbol{x}) - 4\pi I_b(\boldsymbol{x})] \quad ; \quad U(\boldsymbol{x}) = \int_{4\pi} I(\boldsymbol{x}, \boldsymbol{s}')d\boldsymbol{s}' \tag{7}$$

The radiative transfer equation (RTE) for an absorbing, emitting and scattering medium is

$$s.\nabla I_\lambda = -\kappa(\boldsymbol{x},\lambda)I_\lambda(\boldsymbol{x},\boldsymbol{s}) - \sigma_s(\boldsymbol{x},\lambda)I_\lambda(\boldsymbol{x},\boldsymbol{s}) + B(\boldsymbol{x},\lambda) + \frac{\sigma_s(x,\lambda)}{4\pi}\int_{4\pi} \boldsymbol{\Phi}(\boldsymbol{s}',\boldsymbol{s})I(\boldsymbol{x},\boldsymbol{s}')d\boldsymbol{s}' \tag{8}$$

where $\Delta h_{f,\alpha}$ is the heat of formation of species α, $\kappa(\boldsymbol{x})$ is the absorption coefficient, $U(\boldsymbol{x})$ is the integrated radiative intensity, $I_b(\boldsymbol{x})$ is the radiation source term, $I(\boldsymbol{x},\boldsymbol{s})$ is the radiative intensity, $I_\lambda(\boldsymbol{x},\boldsymbol{s})$ is the radiative intensity at wavelength λ, $\boldsymbol{s}$ is the direction vector of the intensity, $\kappa(\boldsymbol{x},\lambda)$ and $\sigma_s(\boldsymbol{x},\lambda)$ are the local absorption and scattering coefficients, respectively and $B(\boldsymbol{x},\lambda)$ is the emission source term, describing how much heat is emitted by the local mixture of gas, soot and droplets/particles.

2.3 Turbulence model and solution procedure

The governing equations for LES are derived by applying a low pass-filter, parameterized by a local cell size δx. They are approximated using second-order accurate finite differences on a three- dimensional grid. Thus, the scalar quantities are assigned to the center of each control volume, the velocity components on their respective faces, and the vorticity components at the edges of the cells. These variables advance in time using an explicit second-order predictor scheme (McGrattan *et al*., 2018a).

The filtered LES equations are simulated using the Deardorff's model to obtain the turbulent viscosity. The diffusion gradient is used by the FDS as a turbulence model to close the subgrid-scale momentum and scalar flux terms. Turbulent diffusivity can be obtained through the constant Schmidt number for mass diffusivity or through the Prandtl number for thermal diffusivity. A more detailed description of the software, equations and models can be found in McGrattan *et al*. (2018a).

2.4 Problem statement

The first objective of this study is to reproduce computationally part of the experimental fire scenarios studied by Johansson *et al*. (2015), using the Fire Dynamics Simulator (FDS) software, in its version 6.7.0, to verify the software's ability to predict this type of fire scenario. Subsequently, the heat source will be positioned against a wall and in the corner of the room (at the floor level), in order to analyze the influence of its location on the HGLT. These positions were chosen due to their strong influence on fire, already identified in other studies presented by Karlsson and Quintiere (2000) and more recently by Lemmertz et al. (2018).

Johansson *et al*. (2015) conducted small-scale experiments in two rooms of different sizes connected by one door and opened to the external environment through a second door. The multi-compartment was built of calcium silicate 12 mm thick and the joints were sealed with a heat resistant inorganic polymerized silicate. The experiment was placed on 24 mm thick chipboard. The calcium silicate boards have a density of 870 kg/m³, heat capacity of 1130 J/kg·K and heat conduction coefficient of 0.175 W/m·K.

The sizes of the openings were varied throughout the experiment. Both rooms had thermocouple trees placed near the corners of the rooms. The fire source was positioned in the center of the inner room (called fire room), consisting of a sandbox burner of 0.1 × 0.1 m². Figure 1 shows the dimensions of the two rooms, as well as the size of the openings, the positions of the fire source and the location of the thermocouple trees used to obtain the temperature readings at each point (dimensions in meters).

As in the experiments, the numerical study will be carried out using methane as fuel, with heat release rates (HRR) of 10 kW and 20 kW, which will be kept constant. The initial ambient temperature (T_{amb}) of the experiments was 28 ºC, being this temperature applied in the calculation of temperature increase ($\Delta T_U = T_U - T_{amb}$). The pressure was 1 atm (101.325 kPa) for all scenarios. Room sizes, variations in openings and HRRs used in each fire scenario are summarized in Tab. 1.

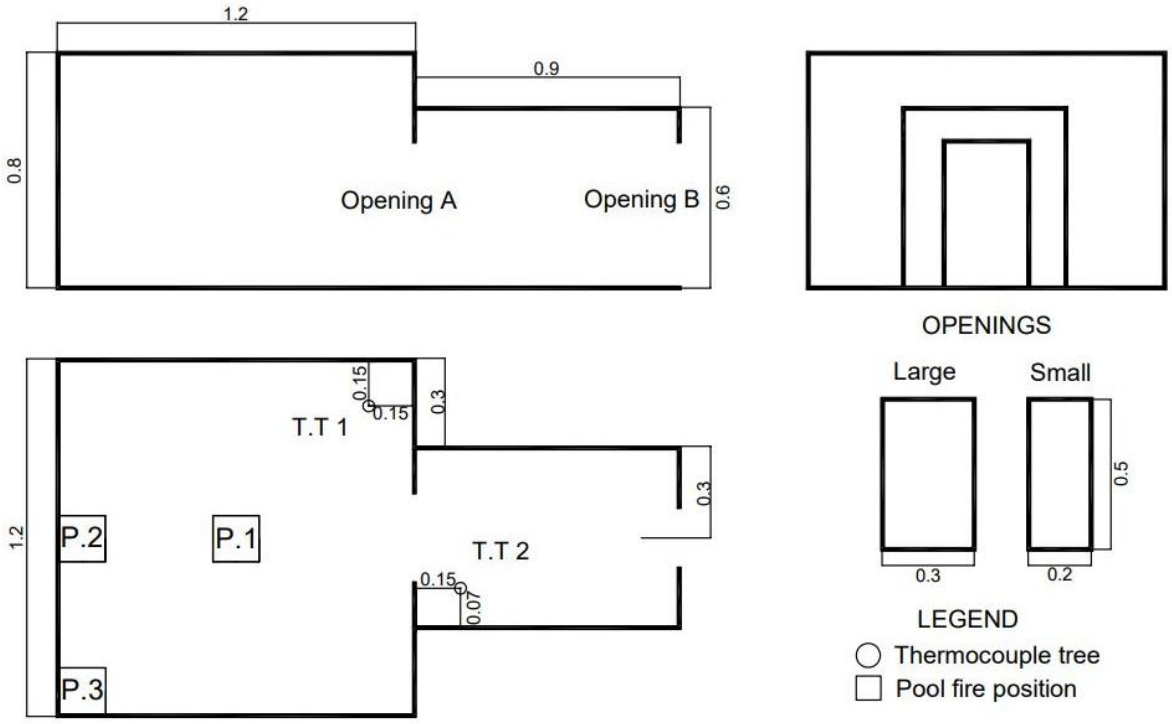

Figure 1. Configuration of the experimental setup (dimensions in meters). Adapted from: Johansson *et al.* (2015).

The thermocouple trees (T.T) were equipped with type K thermocouples; the number of devices varied according to each tree. The vertical position of each thermocouple was measured from the floor. Table 2 shows the heights of each thermocouple in meters.

Table 1. Scenarios description. Adapted from: Johansson *et al*. (2015).

Scenario	Room configuration		Opening type		HRR	
	Fire room	Adjacent room	Opening A	Opening B	20 kW	10 kW
1	Large	Small	Large	Small	X	X
2	Large	Small	Small	Large	X	X
3	Large	Small	Small	Small		X

Table 2. Vertical position of thermocouples. Adapted from: Johansson *et al*. (2015).

Thermocouple Nº	1	2	3	4	5	6	7	8	9	10
T.T 1	0.06	0.15	0.24	0.33	0.45	0.55	0.63	0.73	-	-
T.T 2	0.07	0.11	0.17	0.23	0.29	0.35	0.41	0.46	0.53	0.57

The values referring to experimental measurement uncertainties were calculated by Johansson *et al*. (2015), obtaining the value of 12% for the Hot Gas Layer Temperature.

2.4.1 HGL temperature calculation

The hot gas layer temperature (T_U) is post-processed using the temperature measurements obtained experimentally with the thermocouples, which are also obtained with FDS (temperature readings are obtained from the simulations for the same positions that the temperature was obtained experimentally, as shown in Fig. 1 and Tab. 2). The following equations are employed to post-process T_U:

$$I_1 = \int_0^H T(z)dz = (H - Z_{int})T_U + Z_{int}T_L \tag{9}$$

$$I_2 = \int_0^H \frac{1}{T(z)}dz = (H - Z_{int})\frac{1}{T_U} + Z_{int}\frac{1}{T_L} \tag{10}$$

$$Z_{int} = \frac{T_L(I_1 I_2 - H^2)}{I_1 + I_2 T_L{}^2 - 2T_L H} \tag{11}$$

$$(H - Z_{int})T_U = \int_{Z_{int}}^H T(z)dz \tag{12}$$

where T_L is the lowest thermocouple temperature, $z = 0$ and $z = H$ are the height of the thermocouples closest to the floor and the ceiling, respectively, T_U is the average Hot Gas Layer Temperature and Z_{int} is the layer interface height.

According to Janssens and Tran (1992), Eq. (9) is a mathematical averaging procedure, but without a physical meaning, and Eq. (10) is a requirement for mass equivalency. Combining Eq. (9) and Eq. (10), an expression is obtained to determine the thickness of the smoke layer, Eq. (11). Finally, to determine the Hot Gas Layer Temperature, an average of upper layer temperatures is performed, Eq. (12).

2.5 Mesh resolution

The choice of the mesh that will be used to discretize the domain in a numerical study is of fundamental importance. It must be ensured that the mesh used does not affect the results obtained, taking into account, in addition to the criteria related to the mesh resolution, the computational time and cost, seeking a balance between both parameters.

According to McGrattan *et al*. (2018b), a good way to determine a minimum suitable mesh for modeling fire plumes is through the non-dimensional expression $D^*/\delta x$, where D^* is a characteristic fire diameter (Eq. 13) and δx is the size of a mesh control volume. Values of $D^*/\delta x$ between 4 to 16 have been suggested by a validation study conducted by Salley and Kassawara (2007) and sponsored by the US Nuclear Regulatory Commission. McDermott (2010) points out that a value of $D^*/\delta x$ of the order of 10 has been considered an adequate grid resolution.

$$D^* = \left(\frac{\dot{Q}}{\rho_\infty T_\infty c_p \sqrt{g}}\right)^{2/5} \tag{13}$$

where $\dot{Q}$ is the heat release rate in kW, ρ_∞ is the specific mass of the ambient fluid in kg/m^3, T_∞ is the ambient fluid temperature in K, c_p is the fluid specific heat in kJ/(kg·K) and g is the acceleration of gravity in m/s^2.

The measure of turbulence resolution (MTR) was also calculated to assess and assist in choosing the most suitable mesh. The measure of *M* range between 0 and 1, which according to Pope (2004), must be less than or equal to 0.2, where this value corresponds to 80% resolution of the turbulent kinetic energy. McDermott *et al*. (2010) showed that maintaining MTR values near to 0.2 provides good results, within experimental error bounds, for mean velocities and species concentrations in non-reacting, buoyant plumes.

$$M(x) = \frac{\langle k_{sgs} \rangle}{\langle TKE \rangle + \langle k_{sgs} \rangle} \tag{14}$$

$$TKE = \frac{1}{2}(u_i - \langle u_i \rangle)(u_i - \langle u_i \rangle) \tag{15}$$

where the turbulent kinetic energy per unit mass (TKE) is given by Eq. (15), the subgrid kinetic energy (k_{sgs}) is obtained direct from the FDS, u_i is the cell centered velocity vector from the velocity components at cell faces, the angled brackets denote time-averaged values and subscript *i* indicate grid indices.

To guarantee greater computational precision, without compromising computational efficiency, the computational domain was extended beyond the physical walls in the direction perpendicular to the vertical external opening; so the domain was extended by the value of a hydraulic diameter, as indicated by Zhang X. *et al*. (2010). Table 3 presents the studied meshes and their characteristics, the values of $D^*/\delta x$, the average MTR, the computational time and the relative cost for scenario 1. As can be seen, the $D^*/\delta x$ values for meshes 3, 2 and 1 are within the recommended values for the evaluated HRR's, and mesh 2 presented values close to those recommended by McDermott *et al*. (2010). Analyzing the MTR values, it can be seen that mesh 1 present MTR values below 0.2 and mesh 2 present values close to 0.2.

Table 3. Mesh resolution study values for scenario 1.

Mesh	**Fire room**	**Adjacent room**	**D*/δx**		**Nº Elements**	**Average MTR**	**Computational Time (h)**	**Mesh relative cost**
			HRR (kW)					
			10	**20**				
6	6 cm		2.54	3.35	16128	0.393	0.93	0.01
5	5 cm		3.05	4.02	25200	0.39	1.95	0.02
4	4 cm		3.81	5.03	46376	0.37	4.8	0.04
3	3 cm		5.08	6.7	104632	0.271	12.46	0.1
2	2 cm		7.62	10.06	317504	0.213	57	0.48
1	2 cm	1 cm	7.62 / 15.24	10.06 / 20.10	640256	0.172	119.84	1

In order to better assess the influence of the mesh on the results, a mesh sensitivity study was carried out. Table 4 presents the results of MTR and the increase of the HGLT (ΔT_U) for different meshes, comparing them with the average experimental results, scenario 1 was evaluated with the heat release rate of 10 kW, which has the lowest $D^*/\delta x$ values.

Table 4. Mesh sensitivity analysis for scenario 1 with the HRR of 10 kW.

Mesh	**ΔT_U at the Fire room**				**ΔT_U at the Adjacent room**			
	Experimental data	**Numerical results**	**Relative deviation %**	**MTR**	**Experimental data**	**Numerical results**	**Relative deviation %**	**MTR**
6	152 (150–153)	136.5	10.2	0.314	82 (74–89)	89.1	8.6	0.472
5		138.4	9.0	0.338		88.4	7.8	0.442
4		136.8	10.0	0.321		92.9	13.3	0.419
3		138.8	8.7	0.253		80.6	1.7	0.289
2		144.4	5.0	0.184		83.6	2.0	0.242
1		152.7	0.5	0.183		83.8	2.2	0.160

Comparing the results of meshes 1 and 2, it is noticed that there is a small variation in the results for a large increase in computational cost. Thus, taking into account the good agreement between experimental and numerical values, and highlighting the fact that the MTR is slightly above the indicated value, it was considered that mesh 2 is adequate for carrying out this study. To validate this study, ΔT_U values obtained numerically were compared with the experimental data of scenarios 1, 2 and 3, for the HRRs of 10 kW and 20 kW, in the times of 600 s and 900 s, as shown in Table 5.

Table 5 shows the scenarios and the comparison of numerical and experimental data, where the relative deviation is in relation to the average ΔT_U value and the accuracy in relation within the range of experimental data provided, being a scenario considered with 100% of accuracy when the value lies within the given range.

Table 5. Comparison between experimental data from Johansson *et al*. (2015) and numerical data from FDS (ΔT_U).

Time	Scenario	HRR (kW)	Fire room				Adjacent room			
			Experimental data	ΔT_U	Relative deviation %	Accuracy %	Experimental data	ΔT_U	Relative deviation %	Accuracy %
600s	1	20	244 (236–255)	240.7	1.3	100	118 (108–129)	131.4	11.4	98.1
		10	152 (150–153)	144.4	5.0	96.3	82 (74–89)	83.6	2.0	100
	2	20	244 (243–246)	243.1	0.4	100	105 (104–107)	110.5	5.2	96.7
		10	157 (153–162)	153.7	2.1	100	73 (72–74)	70.3	3.8	97.6
	3	10	161 (155–173)	153.9	4.4	99.3	74 (69–74)	78.1	5.6	94.4
900s	1	20	253 (247–262)	260.4	2.9	99.4	127 (117–139)	145.2	14.3	95.5
		10	161 (158–165)	155.9	3.2	98.7	88 (82–95)	89.8	2.1	100
	2	20	261 (256–267)	268.3	2.8	99.5	113 (110–115)	123.1	8.9	92.9
		10	169 (163–172)	164.0	3.0	100	81 (78–86)	78.2	3.4	100
	3	10	170 (165–179)	165.2	2.8	100	80 (74–85)	86.3	7.8	98.5

Evaluating the validation results presented in Table 5, it can be concluded that the results have a good agreement with the experimental data, presenting one value above the error estimated by Johansson *et al*. (2015), but with an accuracy of 95.5%. Thus, it is considered that a FDS is capable of predicting the hot gas layer temperature for this type of fire in multiple rooms, validating the numerical model for this purpose.

3. RESULTS: INFLUENCE OF FIRE SOURCE POSITION ON THE HGLT

The influence of the position of the heat source on the HGLT was analyzed placing the pool fire parallel to a wall and at the intersection between two walls (corner), keeping them at the floor level, as described in section 2.4 and illustrated in Fig. 1 (P1: center, P2: wall, P3: corner). Table 6 shows the ΔT_U in the fire room and in the adjacent room for each of the studied positions and scenarios.

Table 6. ΔT_U in the fire and adjacent rooms for different fire position.

Time	Scenario	HRR (kW)	ΔT_U in the fire room			ΔT_U in the adjacent room		
			Center (P.1)	Wall (P.2)	Corner (P.3)	Center (P.1)	Wall (P.2)	Corner (P.3)
600s	1	20	240.7	247.9	241.4	131.4	117.1	119.5
	2		243.1	252.2	250.2	110.5	102.7	110.5
	1	10	144.4	152.4	173.5	83.6	78.8	63
	2		153.7	155.6	174.1	70.3	68.1	56.9
	3		153.9	154.6	173.1	78.1	75	61
900s	1	20	260.4	269.1	263.2	145.2	136.3	131.5
	2		268.3	271.8	268.7	123.1	110.7	120.4
	1	10	155.9	165.4	187.1	89.8	83.5	70.4
	2		164	167.7	186	78.2	77.1	62.7
	3		165.2	166.4	188.9	86.3	82.1	67.2

3.1. Fire source positioned in the center

Evaluating the results of Tab. 6 for the pool fire positioned in the center of the room (P.1), the influence of the size of the opening in ΔT_U is perceived. In both scenarios, a larger ΔT_U is noted when the small opening was used in the fire room or in the adjacent room. This behavior can be explained by the reduction of air entrainment in the compartments. When the ventilation of the fire room is reduced, there is an increase in the mixture between the hot and cold gas layer, which results in an increase in the temperature of the cold gases that are entrained by the fire plume, raising the temperature of the Hot Gas Layer. In the adjacent room, reducing the opening leads to an increase in the Hot Gas Layer thickness, which combined with the HGLT, generates an increase in the temperature of the hot and cold gas layer.

It was also noted that in scenario 1 with the pool fire positioned in the center of the room (P.1), the highest ΔT_U was observed in the adjacent room and the lowest ΔT_U was observed in the fire room, as can be seen in Fig. 2. This was due to the relation between the size of openings employed and the position of the fire. The larger ventilation of the fire room (large opening) allows a greater flow of fluid in and out of it. This associated with the fire positioned in the center of the room, allows more air to arrive and be entrained by the plume, which leads to a decrease in the Hot Gas Layer Temperature and increases its thickness. The adjacent room has a small opening connecting it to the outside, so the flow of fluid out and into the room is smaller, which leads to an increase in the HGL thickness, resulting in an increase in ΔT_U in the adjacent room.

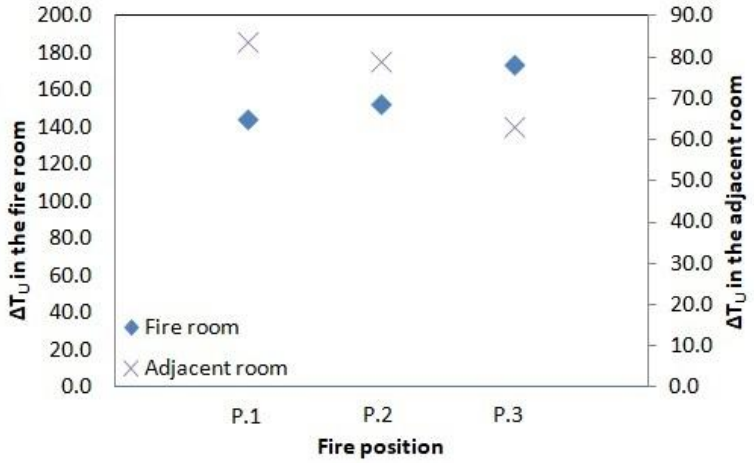

Figure 2. Influence of the heat source position in the ΔT_U in scenario 1 with the HRR of 10 kW at 600s.

3.2. Fire source positioned near a wall

When positioning the pool fire parallel to a wall (P.2), the temperature of the smoke layer of the fire room tends to increase and its thickness decreases. This behavior occurs due to the air restriction imposed by the wall, which reduces the air entrained by the plume. In this way, the thickness of the smoke layer in the adjacent room will also be smaller, as well as its temperature, due to the thermal exchanges between the smoke layer and the surroundings.

Evaluating the results of ΔT_U for the fire source near a wall (P.2) presented in Fig. 3-a, it is observed the proximity of the values, even with different openings in the fire room. In scenarios 2 and 3, there was only a small increase in ΔT_U in the fire room when the fire was near a wall, compared to the fire placed in the center (P.1), whereas in scenario 1 this variation was greater. This behavior is due to the limitation of air entrainment caused by the walls, making the ventilation of the room to have a lesser influence on the HGLT in the fire room. The small ΔT_U variation between scenarios 2 and 3 in any given fire source position is due to the small opening of the fire room, which allowed a smaller amount of air to enter the room and reach the plume.

In the adjacent room, the ΔT_U values showed a greater difference between different scenarios, even with the HGLT values of the fire room close in all scenarios, as can be seen in Fig 3-b. These differences occur due to the openings used in both rooms. Scenario 1 has the highest ΔT_U values due to the large opening in the fire room and the small one in the adjacent room, as already explained, and scenario 2 the lowest ΔT_U values because of the small opening in the fire room and the large in the adjacent room, having a behavior opposite to that of scenario 1.

3.3. Fire source positioned in a corner

The results for the pool fire positioned at the intersection between two walls (P.3) are shown in Fig. 3-a and Fig. 3-b, they show that there is an increase in the HGLT in the fire room in relation to positions P.1 and P.2. This expected

behavior occurs due to the air restrictions imposed on the plume by the presence of the walls, reducing the air entrainment. As observed in position P.2, the ΔT_U values in the fire room are similar, regardless of the scenario analyzed, making it more evident that with the limited air entrain imposed by the walls, there is less influence of ventilation on ΔT_U in the fire room.

The ΔT_U values in the adjacent room are the lowest in relation to the other two fire source positions. This is a result of the limitation of the air entrain into the plume, resulting in a lower volume of smoke, decreasing the HGL thickness.

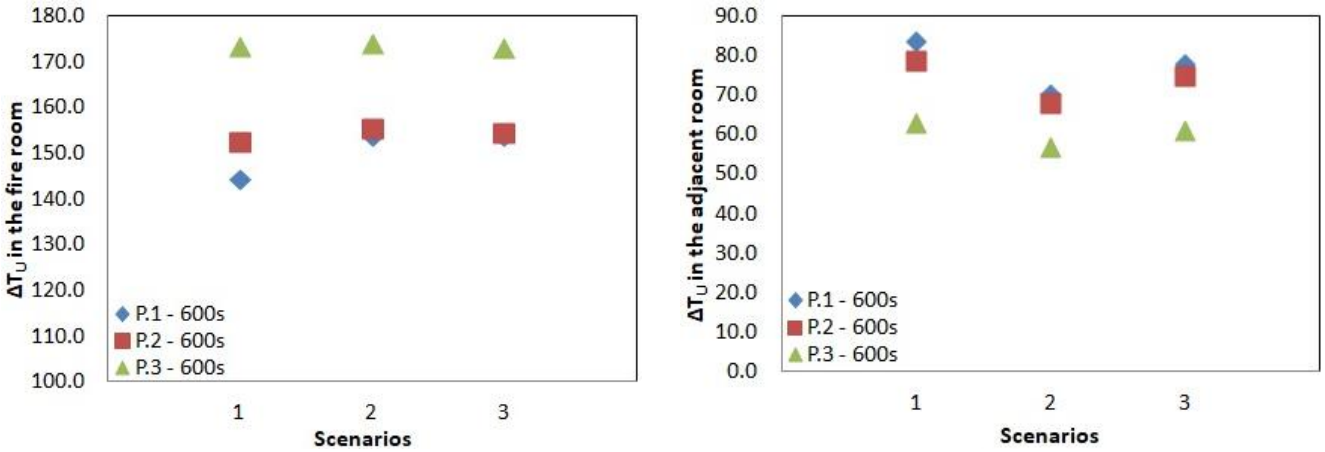

a) Fire room b) Adjacent room

Figure 3. Influence of the heat source position in the ΔT_U in the a) fire room and in the b) adjacent room with the HRR of 10 kW.

3.4. Heat Release Rate influence

As can be seen in Tab. 6, with the increase in HRR, there is an increase in ΔT_U values in both rooms and for all positions. This is the expected behavior, as the HRR represents a certain amount of energy released per unit of time. However, an atypical behavior can be seen in P.3 for the HRR of 20 kW. It was expected that fires near corners would provide values higher than those found for fires near walls, as was predicted using the HRR of 10 kW, but this result was not obtained. It is assumed that the increase in air circulation in the room has affected the temperature reading locations, which may have happened due to the increase in HRR and the consequent increase in the mass flow in the room, being necessary to investigate the cause of this discrepancy in future studies.

4. CONCLUSIONS

In this study, numerical simulations were carried out using FDS, in order to evaluate the software capacity to reproduce fires in multi-compartments and to analyze the influence of the fire source location on the Hot Gas Layer Temperature in this type of environment.

The numerical model showed a good agreement between the results obtained and the experimental data, when using the mesh defined through the mesh resolution study.

The results of the study showed that when placing the pool fire next to a wall or in a corner of the room, there is an increase in the HGLT in the fire room and a decrease in the thickness of the smoke layer due to the reduction of the air entrainment. In the adjacent room, this decrease in the thickness of the smoke layer leads to a reduction in the HGLT of the environment, due to the thermal exchanges with the surroundings.

Thus, the highest HGLT found in the fire room occurred with the pool fire positioned in the corner of the room, P.3, not suffering major influence of the room opening. The scenario that presented the highest HGLT in the adjacent room was scenario 1, with the pool fire positioned in the center, P.1.

5. ACKNOWLEDGEMENTS

This study was financed in part by the Coordenação de Aperfeiçoamento de Pessoal de Nível Superior - Brasil (CAPES) - Finance Code 001.

Author F. R. Centeno thanks National Council for Scientific and Technological Development (CNPq).

6. REFERENCES

Betting, B., Varea, E., Gobin, C., Godard, G., Lecordier, B., Patte-Rouland, B., 2019. "Experimental and numerical studies of smoke dynamics in a compartment fire". *Fire Safety Journal*, Vol. 108.

Haouari-Harrak, S., Mehaddi, R., Boulet, P., Koutaiba, E.M., 2020. "Evaluation of the room smoke filling time for fire plumes: Influence of the room geometry". *Fire and Materials*.

Janssens, M., and Tran, H. C., 1992. "Data Reduction of Room Tests for Zone Model Validation*". Journal of Fire Sciences*, Vol. 10, No. 6, pp. 528–555.

Johansson, N., Svensson, S., and Van Hees, P., 2015. "An evaluation of two methods to predict temperatures in multi-room compartment fires". *Fire Safety Journal*, Vol. 77, No. 77, pp. 46–58.

Karlsson, B., and Quintiere, J. G., 2000. "*Enclosure fire dynamics*". Boca Raton, Florida, CRC Press LLC.

Lemmertz, C.K., Centeno, F.R., Arnswaldt, W.J.V., Beshir, M., Rush, D., 2018." An analysis of the influence of the fire source location on the hot gas layer temperature in a pre-flashover compartment fire *In Proceedings of the 17th Brazilian Congress of Thermal Sciences and Engineering* - ENCIT 2018. Águas de Lindóia, SP, Brazil.

Marchetti, L. J., 2012. "*Fire Dynamics Series: Predicting Hot Gas Layer Temperature and Smoke Layer Height in a Room Fire with Natural and Forced Ventilation*." PDHonline Course.

McDermott, R. J., Forney, G. P., McGrattan, K., and Mell, W. E., 2010. "Fire Dynamics Simulator version 6: complex geometry, embedded meshes, and quality assessment". *In V European Conference on Computational Fluid Dynamics*, ECCOMAS CFD, pp. 14–17. Lisbon, Portugal.

McGrattan, K., Hostikka, S., McDermott, R., Floyd, J., Vanella, M., Weinschenk, C., and Overholt, K., 2018a. "*Fire Dynamics Simulator Technical Reference Guide Volume 1: Mathematical Model*." NIST Special Publication. Gaithersburg, MD, 6th edition.

McGrattan, K., Hostikka, S., McDermott, R., Floyd, J., Vanella, M., Weinschenk, C., and Overholt, K., 2018b. *Fire Dynamics Simulator User's Guide*. NIST Special Publication, Gaithersburg, MD, 6th edition .

Pope, S. B., 2004. "Ten questions concerning the large-eddy simulation of turbulent flows". *New Journal of Physics*, Vol. 6.

Sahu, D., Kumar, S., Jain, S., Gupta, A., 2017. "Full scale experimental and numerical studies on effect of ventilation in an enclosure diesel pool fire". *Building Simulation*, Vol. 10, pp. 351–364.

Salley, M.H., Kassawara, R.P., 2007. "*Verification and Validation of Selected Fire Models for Nuclear Power Plant Applications, Volume 7: Fire Dynamics Simulator (FDS)*". U.S. Nuclear Regulatory Commission, Office of Nuclear Regulatory Research (RES), Rockville, MD, and Electric Power Research Institute (EPRI), Palo Alto, CA, NUREG-1824 and EPRI 1011999.

Tlili, O., Mhiri, H., and Bournot, P., 2016. "Empirical correlation derived by CFD simulation on heat source location and ventilation flow rate in a fire room". *Energy and Buildings*, Vol. 122, p. 80–88.

Węgrzyński, W., Konecki, M., 2018. "Influence of the fire location and the size of a compartment on the heat and smoke flow out of the compartment". *AIP Conference Proceedings* 1922, 110007.

Zhang, X., Yang, M., and Wang, J., 2010. "Effects of Computational Domain on Numerical Simulation of Building Fires". *Journal of fire protection engineering*, Vol. 20, pp. 225 – 251.

7. RESPONSIBILITY NOTICE

The authors are the only responsible for the printed material included in this paper.